Journal Homepage: https://dergipark.org.tr/tr/pub/isibted

Isı Bilimi ve Tekniği Dergisi

Archive: https://tibtd.org.tr/dergi

Influence Of The Enhanced Tubes For Steam Condensation On Horizontal Tube Bundle In The Absorption Chiller

Abdolkarim MOHAMMADZADEH [1], Mohammadhasan Jalaleddin ABYANEH [1,*], Farzad JAFARKAZEMİ [1]

[1] *Department of Mechanical Engineering, South Tehran Branch, Islamic Azad University, Tehran, Iran.*

A R T I C L E I N F O

2025, vol. 45, no.2, pp. 317-324

doi: 10.47480/isibted.1689365

Research Article
Received: 07 May 2025
Accepted: 08 September 2025

* *Corresponding Author*
e-mail: mhj_abyaneh@azad.ac.ir

Keywords:
Heat Exchanger,
Horizontally Oriented Condensers,
Computational Fluid Dynamics,
Simple Tube,
Tube with External Fin,
Tube with Internal Groove.

ORCID Numbers in author order:
0009-0000-2485-2409
0000-0000-0000-0000
0000-0002-8840-3810

A B S T R A C T

This work presents the numerical analyses for condensation of steam outside the horizontal tube bundle in the absorption chiller. The objective of this paper was to numerically compare the effect of three different types of horizontal tube bundles on different heat transfer parameters of the absorption chiller. For this purpose, three types of tubes, including a simple tube, a tube with external fins, and a tube with internal grooves, were analyzed. Two-equation turbulence models have been used to simulate the flow field and heat transfer and the finite volume method was applied for numerical analyses using CFX software. The results showed that adding external fins or an inner groove to the tube increased the heat transfer coefficient of the tube bundle in the absorption chiller. Due to the increase in heat transfer in condensers equipped with finned and grooved tubes, the rate of steam condensation in these heat exchangers was higher. The percentage of outlet condensate in the condenser with finned and grooved tubes was approximately 4.8 times that of the heat exchanger with a simple tube. In conclusion, the overall findings indicated the increased performance of the condenser for the horizontal oriented tube bundles with external fin and internal groove.

Absorpsiyonlu Soğutucuda Buhar Yoğuşması İçin Geliştirilmiş Boruların Yatay Boru Demetine Etkisi

M A K A L E B İ L G İ S İ

Anahtar Kelimeler:
Su kaynaklı ısı pompası
Al_2O_3
Enerji analizi
Ekserji analizi
Yaşam döngüsü iklim performansı

Ö Z E T

Bu çalışma, absorpsiyonlu soğutucuda yatay boru demetinin dışındaki buharın yoğuşması için sayısal analizleri sunmaktadır. Bu makalenin amacı, üç farklı tipteki yatay boru demetinin absorpsiyonlu soğutucunun farklı ısı transfer parametreleri üzerindeki etkisini sayısal olarak karşılaştırmaktır. Bu amaçla, basit boru, harici kanatçıklara sahip boru ve dahili oluklara sahip boru olmak üzere üç tip boru analiz edilmiştir. Akış alanını ve ısı transferini simüle etmek için iki denklemli türbülans modelleri kullanılmış ve CFX yazılımı kullanılarak sayısal analizler için sonlu hacim yöntemi uygulanmıştır. Sonuçlar, boruya harici kanatçıklar veya dahili oluk eklenmesinin absorpsiyonlu soğutucudaki boru demetinin ısı transfer katsayısını artırdığını göstermiştir. Kanatçıklı ve oluklu borularla donatılmış kondenserlerde ısı transferindeki artış nedeniyle, bu ısı değiştiricilerdeki buhar yoğuşma oranı daha yüksek olmuştur. Kanatçıklı ve oluklu borulara sahip kondenserdeki çıkış kondens yüzdesi, basit borulu ısı değiştiricinin yaklaşık 4,8 katı olmuştur. Sonuç olarak, genel bulgular, dış kanatçıklı ve iç kanallı yatay boru demetleri için kondenserin performansının arttığını göstermiştir.

NOMENCLATURE

c_p	Thermal capacity ($J.kg^{-1}.K^{-1}$)	Q	Heat flux (W)
D_o	Tube outer diameter (m)	q	Surface heat flux ($W.m^{-2}$)
f	Friction factor	R	Tube outer radius (m)
F_d	Tube spacing parameter	r	Radial coordinate from the surface of the surface (m)
g	Gravitational acceleration ($m.s^{-2}$)	S	Heat transfer surface (m^2)
H_f	Enthalpy flow rate per unit length ($W.m^{-1}$)	T	Temperature (K)
H	Heat transfer coefficient ($W.m^{-2}.K^{-1}$)	U	Vapor orthoradial velocity ($m.s^{-1}$)
Δh_v	Phase change enthalpy ($J.kg^{-1}$)	u	Condensate orthoradial velocity ($m.s^{-1}$)
J	Condensation mass flux ($kg.s^{-1}.m^{-2}$)	V	Vapor radial velocity ($m.s^{-1}$)
n	Tube row number	v	Condensate radial velocity ($m.s^{-1}$)
p_t	Tube pitch (m)	ρ	Density ($kg.m^{-3}$)
p	Pressure (Pa)		

INTRODUCTION

Heat exchangers are widely used to transfer heat between two or more fluids at different temperatures, and they are commonly applied in various applications (such as air conditioning systems, refrigeration, and power systems engineering) (Popov et al., 2019). Therefore, increasing heat transfer between steam and cooling tubes has always been of interest for different industries and numerous studies were devoted to design and manufacturing the heat exchangers (Dalkilic & Wongwises , 2009). Interest in condensing on the outside of horizontal tubes is increasing due to the demand for higher energy efficiency, lower material costs, and other economic incentives (Rifert & Sereda, 2015; Yang & Shen, 2008; Zhang et al., 2025). Hence, condensation on horizontal tubes has become a commonly applied technique in recent decades.

Two-phase flow is commonly dominated by gravity and vapor shear forces when the condensing system is designed based on inside/outside horizontal tubes. However, annular flow pattern can be associated with increased vapor shear, and slug flows appear when the gravity is used to control the force (Cavallini et al., 2003). Condensation of zeotropic refrigerants in horizontal tubes were investigated using an experimental study (Dobson & Chato, 1998) by measurements in smooth and round tubes with different diameters. In this study a two-phase multiplier approach for annular flow was performed. The results demonstrated that the heat transfer coefficient can increase with accumulative mass flux and enhanced vapor quality in annular flow due to increased shear stress and a thinner liquid film compared to other flow regimes (Dobson & Chato, 1998). In another study (Wongwises & Polsongkram, 2016), the helically coiled concentric tube in tube heat exchanger was tested to evaluate two-phase heat transfer coefficient and the pressure drop as well. This experimental study discovered that the average heat transfer coefficient and the pressure drop of this new designed heat exchanger was increased around 33 to 53% and 29 to 46%, respectively, compared to the conventional straight tube in tube heat exchanger (Wongwises & Polsongkram, 2016). Similar to the aforementioned investigations, abundant research / industrial works have reported the heat transfer characteristics for horizontal oriented condensation (Dalkilic & Wongwises , 2009; García-Valladares, 2003; Chen et al., 2019; Infante Ferreira et al., 2003), which encourages the researchers for extra detailed studies for evaluation of condensation heat transfer mechanism.

With the intention of increasing the efficiency of the condensers, accurate computational modeling can be utilized to predict the thermal and fluid-dynamic behavior in designed system. Numerical simulation is an excellent tool for the design and improvement of the new condensing systems and can be easily used for parametric studies to evaluate different geometrical design parameters (Kharangate & Mudawar, 2017). Computational fluid dynamics (CFD) simulations were previously used (Gebauer et al., 2013) to predict the condensation heat transfer on low finned tubes and the achieved results were in in alignment with experimental data and analytical models. However, although numerical simulations of single-phase flow have revealed tremendous success, modeling two-phase flow with phase change is still restricted to simplified configurations (Kharangate & Mudawar, 2017; Saleh & Ormiston, 2016; Kleiner et al., 2019; Yang et al., 2008; Ghedira et al., 2025). The application of tubes with external fin and internal groove is recently increased for design of industrial condensers. Nonetheless, a comprehensive study to evaluate the effect of tube type for enhancing the efficiency of the condensation outside horizontal tubes have not yet been well documented.

Consequently, this study aimed to numerically compare the effect of three different types of horizontally oriented condensation systems on various heat transfer parameters. For this objective, three types of tube including (1) simple tube, (2) tube with external fin, and (3) tube with internal groove were investigated. A CFD modeling was developed and the flow field and the calculated heat inside and outside of the tube were thoroughly investigated, and the advantages and disadvantages of using the aforementioned tubes were evaluated.

MATERIALS AND METHODS

Geometric Modeling

The geometry of this study was developed using ANSYS Design Modeler (ANSYS Inc., PA, USA). This geometry consisted of three different parts (Figure 1). The first part of the geometry related to the in-tube fluid, where the fluid bulk related to this section has been modeled. The other part was the geometry of the tube wall, which was considered in the solid simulations. The coolant tube geometry was considered in 4 horizontal rows with the length of 340 mm. The outer diameter of the tubes was 50 mm with a thickness of 7 mm. The third part represented the space around the tubes, which corresponds to

the steam chamber along with its fluid bulk. The overall geometry including the length, width and height of this section were extracted from a previous work (Singh et al., 2001), which were 340 mm, 300 mm and 750 mm, respectively (Figure 1). For this study, three types of tube including simple tube (Figure 1A), tube with external fin (Figure 1B), and tube with internal groove (Figure 1C) were developed.

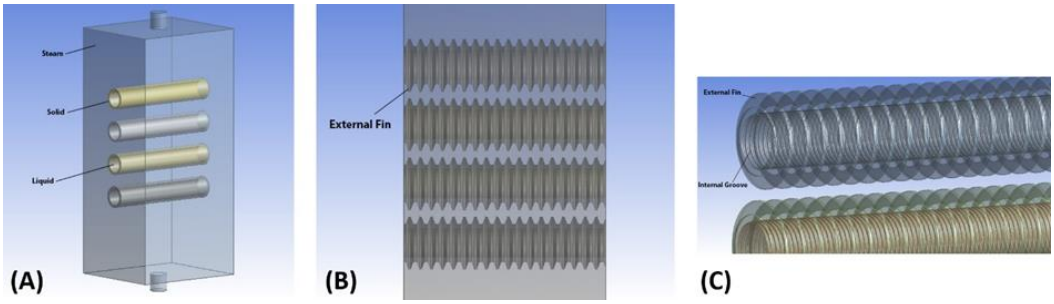

Figure 1. Geometry of the three domains: (A) simple tube, (B) tube with external fins, and (C) tube with external fins and internal grooves. These geometries were used for CFD simulations of horizontal condensation.

Geometry meshing of the developed models (Figure 2A) were performed using ANSYS Meshing software (ANSYS Inc., PA, USA). With the intention of attaining the optimal number of elements, finer elements have been used near the cooling tubes, which have a higher temperature and velocity gradient, and the elements have grown larger away from them. For this purpose, a specific sizing has been determined for each section. This resulted in a higher mesh density in sensitive areas and a lower mesh density in other sections. Tetrahedral elements were used, and to avoid increasing the element aspect ratio, the growth of element size was gradual. Boundary layer elements were also applied for this problem. In order to evaluate the independence of the model response from the number of elements, the problem of the simple tube condenser with three different meshes has been analyzed. For this purpose, the effect of increasing the elements on the calculated heat transfer coefficient for four tubes were compared. In addition, the Skewness technique was used to check the quality of geometry meshing. Figure 2B shows a histogram of the elements percentage distribution for different Skewness values. The average Skewness of the elements used in this study was 0.22.

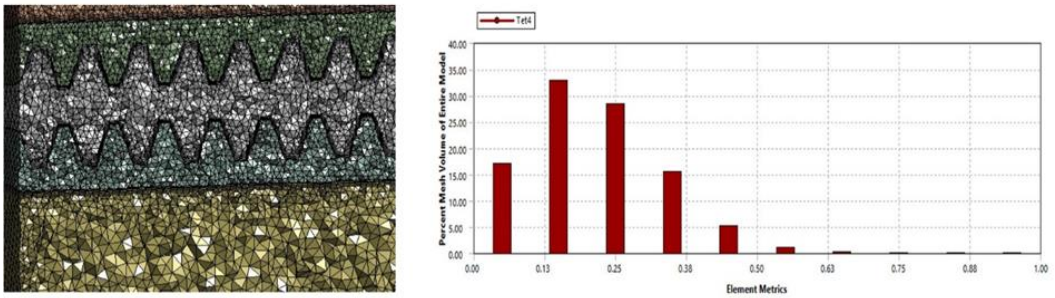

Figure 2. (A) Meshing of the CFD model, showing higher mesh density near the cooling tubes and coarser elements away from the tubes. (B) Histogram of element skewness values to assess mesh quality; average skewness = 0.22.

Model Validation

To assess the validity of the utilized simulations in this study, the Nusselt's theory were examined (Bonneau et al., 2019) to compare the achieved results from analytical and numerical analyses for condensation on a single tube with vapour at rest. The hypotheses for the horizontal tube study can be summarize as follow,

1. The surrounding vapour is at rest and saturated.
2. The wall temperature is uniform and the laminar and purely orthoradial condensate flow around the tube surface could be considered.
3. The shear stress at the liquid and vapour interface can be ignored in the condensate film.
4. The heat is transferred by conduction through the condensate film.
5. The condensate properties are taken during analysis at saturation as well.

Equation of momentum for a two-dimensional stationary purely orthogonal flow within a film is as Eq. 1 and can be obtained as Eq. 3 using the mentioned boundary condition in Eq. 2,

$$v_l \frac{\partial^2 u}{\partial r^2} + g\sin(\theta) = 0 \quad (1)$$

$$\begin{cases} u(r=0) = 0 \ \ (no\ slip\ boundary) \\ \left(\frac{\partial u}{\partial r}\right)_\delta = 0 \ \ (no\ shear\ stress\ at\ vapour - liquid\ interface) \end{cases} \quad (2)$$

$$u(r,\theta) = \frac{g}{2v_l}\sin(\theta)\, r(2\delta - r) \quad (3)$$

Therefore, the mean velocity over the film is as follow,

$$\overline{u} = \frac{1}{\delta}\int_0^\delta u dr = \frac{g}{3v_l}\sin(\theta)\,\delta^2 \quad (4)$$

Considering the mass balance is achieved over a portion of the condensate film (Bonneau et al., 2019), and substituting the equations, the heat transfer coefficient over the tube can be calculated as follow (Eq. 5),

$$\bar{h} = \frac{1}{\pi}\int_0^{\pi} h d\theta = 0.728\left(\frac{\rho_l g \lambda_l^3 \Delta h_v}{\nu_l D_0 \Delta T}\right)^{1/4} \quad (5)$$

The simulations in two different pressures were performed and the calculated heat transfer coefficients were compared with the ones calculated from above-mentioned equation to check the validity.

Numerical Modeling

The first solution domain was related to the in-tube water which was a fluidic solution. The boundary condition at the inlet and outlet of the tubes were flow type and pressure type, respectively. In the simulations, the boundary condition at the inlet and outlet of the tubes were flow type and pressure type, respectively. The inlet vapor velocity was set to 0.1 m/s with temperature equal to 100° C. The outlet pressure was set to 1 bar. The CFD simulations were conducted using a Mixture multiphase model with thermal phase change activated to simulate condensation. The saturation temperature was set to 100 °C, and the interphase heat transfer was modeled using the Two-Resistance approach, with zero resistance for the liquid phase and the Ranz–Marshall correlation for the vapor phase. This setup ensures that the latent heat associated with condensation is accurately captured. While the Mixture model does not explicitly track the interface, it provides a volume-averaged representation of the two-phase flow, which is sufficient to capture the macroscopic condensation dynamics under the flow conditions studied. To ensure fully developed flow at the tube inlet, a portion of the tube was analyzed, and a pre-calculated velocity profile from a validated previous study was applied as the inlet boundary condition. This approach guarantees that the velocity boundary layers are fully developed at the entrance, minimizing flow disturbances and providing accurate predictions of condensation and heat transfer while reducing computational effort. The second solution domain was related to the water vapor which was a fluidic solution, as well. The flow regime was considered as turbulent and the k-ε model was used for fluidic modeling. Gravity acceleration was considered in all of fluid solutions. In this case, the condensation of steam was deliberated in simulations. Hence, a phase change could occur in the water vapor domain solution. The last solution domain was related to the solid tube wall which was made of copper and its heat transfer was evaluated.

The governing equations for the viscous fluid flow in the turbulent state are expressed by the time-averaged Navier-Stokes equations. Using time-averaging of the continuity (conservation of mass) and motion (conservation of momentum), the basic equations are as following equations (Eq. 6 to 8).

$$\rho \frac{\partial U_i}{\partial x_i} = 0 \quad (6)$$

$$\underbrace{\rho U_i \frac{\partial U_j}{\partial x_i}}_{I} = -\underbrace{\frac{\partial P}{\partial x_j}}_{II} - \underbrace{\frac{\partial \tau_{ij}}{\partial x_i}}_{III} + \underbrace{\rho g_j}_{IV} \quad (7)$$

I: Momentum convection
II: Surface force
III: Molecular-dependent momentum exchange (diffusion) where

$$\tau_{ij} = -\mu\left(\frac{\partial U_j}{\partial x_i} + \frac{\partial U_i}{\partial x_j}\right) + \frac{2}{3}\delta_{ij}\mu\frac{\partial U_k}{\partial x_k}$$

IV: Mass force

$$\underbrace{\rho c_\mu U_i \frac{\partial T}{\partial x_i}}_{I} = -\underbrace{P\frac{\partial U_i}{\partial x_i}}_{II} + \underbrace{\lambda\frac{\partial^2 T}{\partial {x_i}^2}}_{III} - \underbrace{\tau_{ij}\frac{\partial U_j}{\partial x_i}}_{IV} \quad (8)$$

I: Convective term
II: Pressure work
III: Heat flux (diffusion)
IV: Irreversible transfer of mechanical energy into hea

Two-equation turbulence models have been extensively used to simulate the flow field and heat transfer in mechanical engineering applications. In this study, the standard k-ε model was used. The governing equations for fluid flow in this model are expressed by following equations (Eq. 9 and 10);

$$K: \frac{\partial(\rho k u_i)}{\partial x_i} = \frac{\partial}{\partial x_j}\left[\frac{\mu_t}{\sigma_k}\frac{\partial k}{\partial x_j}\right] + 2\mu_t E_{ij}E_{ij} - \rho\varepsilon \quad (9)$$

$$\varepsilon: \frac{\partial(\rho\varepsilon u_i)}{\partial x_i} = \frac{\partial}{\partial x_j}\left[\frac{\mu_t}{\sigma_\varepsilon}\frac{\partial \varepsilon}{\partial x_j}\right] + C_{1\varepsilon}\frac{\varepsilon}{k}2\mu_t E_{ij}E_{ij} - C_{2\varepsilon}\rho\frac{\varepsilon^2}{k} \quad (10)$$

Finite volume method was applied for numerical analyses using CFX software (ANSYS Inc., PA, USA). The pre-processing, problem solving and post-processing steps were performed in CFX-Pre, CFX-Solver and CFX-Post sections, respectively.

RESULTS

Based on the meshing sensitivity analyses, increasing the number of elements from 2983010 to 3866178 resulted in less than 0.0003% change in calculated results (Figure 3). Hence, the total number of elements were 2983010 for solving the problems in in this study. The calculated heat transfer coefficients from the model were in good agreement with those calculated from the Nusselt's theory (Figure 4A), which confirmed the validity of this numerical modeling. The difference between the calculated results for the numerical solution and Nusselt formula was 4%.

The inlet profile to the cooling tubes was individually extracted from the achieved result from the simulations of the different tube types. Figure 4B presents the velocity vectors in tubes. The velocity component in the main simulations was choosen based on the values after the flow in the tube has been fully developed. During the solutions, the sensitivity analyses regarding the independence of the results from the number of iterations were performed and verified the accuracy of the model (Figure 5A). The liquid volume fraction parameter, defined as the 'proportion of element space occupied by the liquid phase to all phases,' was monitored at two different points. When this parameter remained constant during the solution, it indicated the convergence of the numerical modeling (Figure 5A). Figure 5B shows the absolute pressure contour in one of the modeled heat exchangers. The pressure throughout the heat exchanger was almost constant but due to the gravity, the pressure at the bottom of the heat exchanger was higher (Figure 5B).

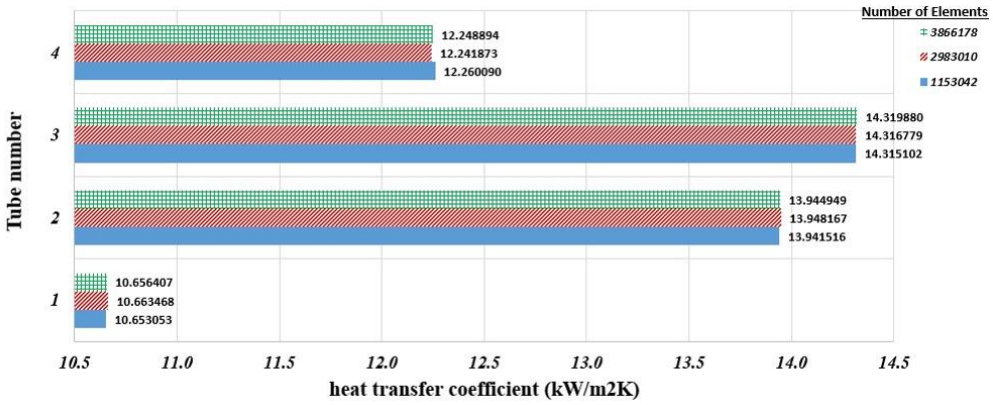

Figure 3. Results of mesh sensitivity analysis, showing the effect of increasing the number of elements on the calculated heat transfer coefficient.

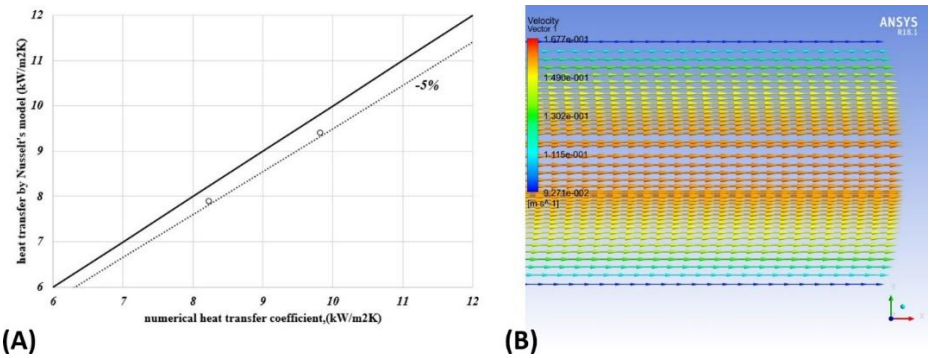

Figure 4. (A) Comparison of the heat transfer coefficient calculated by Nusselt's theory and numerical CFD simulations for validation purposes. (B) Fully developed velocity profiles at the inlet of the cooling tubes for different tube geometries.

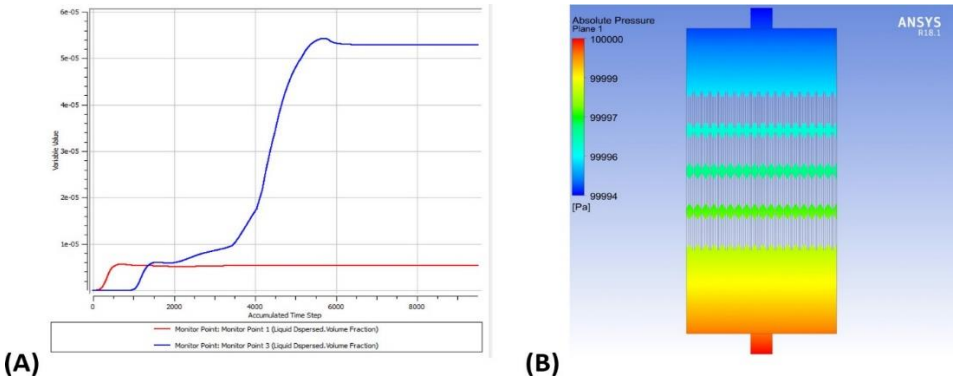

Figure 5. (A) Convergence analysis showing the independence of results from the number of iterations. (B) Absolute pressure contour in the heat exchanger, indicating pressure variation due to gravity along the tube bundle.

The path of steam in the heat exchanger is shown by the streamlines in Figure 6A. The steam rose again after moving downward in the heat exchanger, and this movement repeated periodically (Figure 6A). Furthermore, Figure 6B presents the velocity contour in a plane section. Velocity differences in distinct parts of the heat exchanger resulted in non-uniform steam flow along the walls of the cooling tubes. Consequently, as shown in Figure 6C, the temperature distribution on the walls of the cooling tubes did not exhibit a uniform pattern and was influenced by the scattered movement of steam, which can be investigated by following the streamlines.

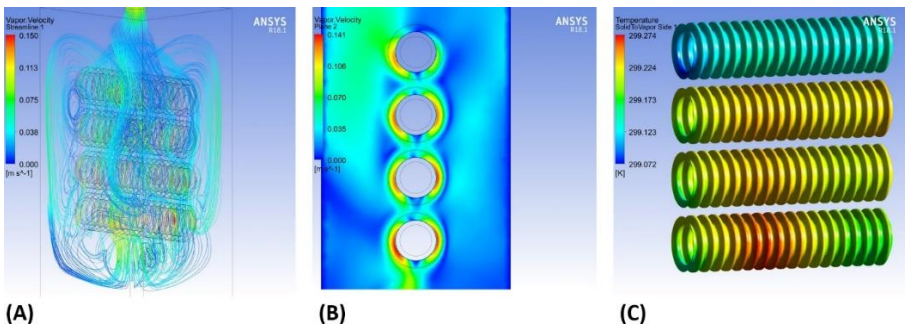

Figure 6. (A) Streamlines of vapor velocity in the heat exchanger, showing the path of steam and recirculation regions. (B) Velocity contour in a plane section, highlighting non-uniform flow along the tube walls. (C) Temperature distribution on the wall of the cooling tubes, showing areas of enhanced heat transfer corresponding to steam movement.

Figure 7A shows a section of the steam temperature contour. The steam temperature was almost constant throughout the heat exchanger, with a temperature decrease observed only at the points of contact with the cooling tubes (Figure 7A). The collision of steam with the walls of the cooling tubes resulted in steam condensation. Figure 7B shows a volumetric view of the condensed liquid volume fraction at the points of contact with the cooling tubes. The acceleration due to gravity caused the condensate to fall onto the lower tubes, which affected the performance of these tubes (Figure 7B). Figure 7C presents the contour of the condensed liquid volume fraction. The increase in the volume fraction of the condensate at lower heights of the heat exchanger was due to this phenomenon (Figure 7C).

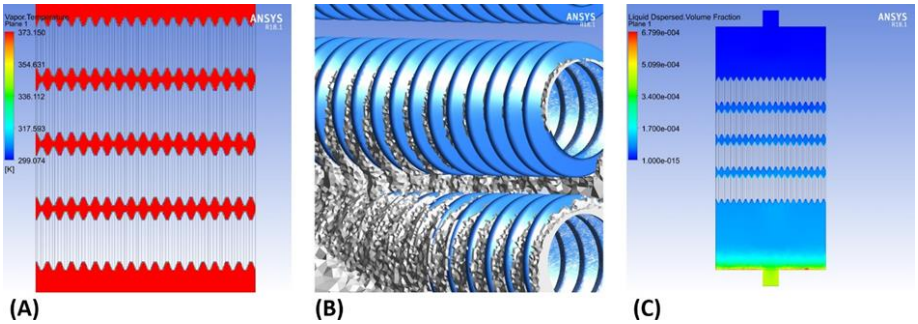

Figure 7. (A) Steam temperature contour in a plane section, indicating uniform temperature except near the tube walls. (B) Volumetric view of the condensed liquid volume fraction at the points of contact with cooling tubes. (C) Contour of the condensed liquid volume fraction in a plane section, showing accumulation of condensate at lower positions due to gravity.

DISCUSSİON AND CONCLUSION

Understanding the effect of tube type for enhancing the efficiency of the condensation outside horizontal tubes is of great value for design of heat exchangers. This study provided a CFD modeling approach of the heat transfer analyses to compare the efficiency of the aforementioned different types of horizontal oriented condensation system. For this purpose, two-equation turbulence models were used to simulate the flow field and heat transfer in the three models. The validity of these numerical simulations was already verified; however, to further validate the findings, future experimental studies will be conducted to compare the CFD results with real-world data, addressing the need for experimental verification.

The main contribution of this study was to compare the performance patterns of three different modeled heat exchangers. Figure 8 compares the heat transfer coefficient outside the tubes for the three types of heat exchangers. The relationship between the heat transfer coefficients of different tubes in these heat exchangers is also presented in Figure 8.

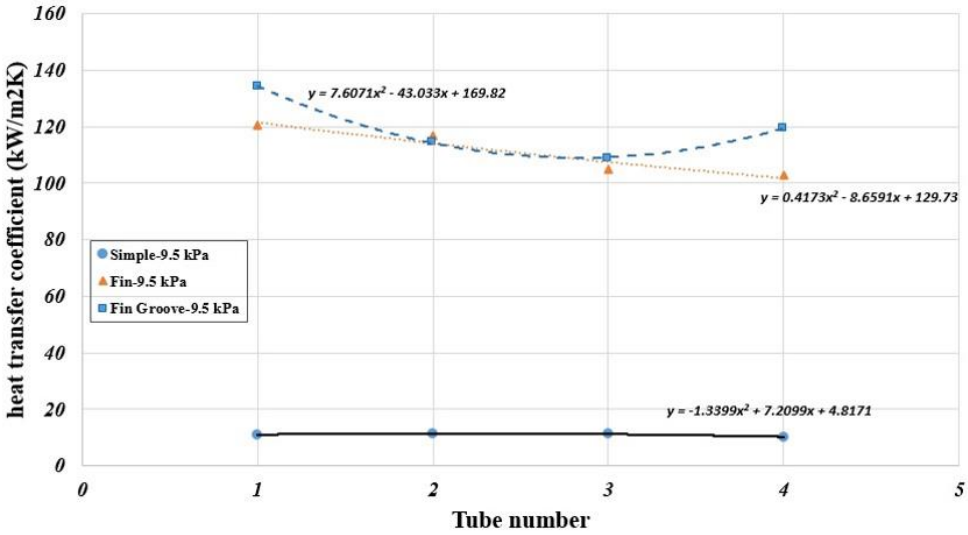

Figure 8. Heat transfer coefficient distribution along the tube exterior for the three types of heat exchangers, comparing simple, finned, and grooved tubes.

Figure 9 compares the average heat transfer coefficient for the three types of heat exchangers. As it was observed, the percentage increase in the heat transfer coefficient parameter was increased 906% for cooling tubes with external fin compared to a simple tube. This percentage was 983% for the tube with internal groove. This showed that adding an inner groove to the tube leads to 77% increase in heat transfer coefficient.

Due to the increase in heat transfer in heat exchangers equipped with finned and grooved tubes, it can be expected that the rate of steam condensation in these heat exchangers is higher, which could be beneficial for designers. The percentage of outlet condensate relative to the total outlet fluid from the heat exchanger was quantified for the three models at 100 kPa, as presented in Figure 10. The percentage of outlet condensate in the heat exchanger with finned and grooved tubes was approximately 4.8 times that of the heat exchanger with a simple tube (Figure 10). Despite these advantages, a drawback of finned and grooved tubes is that pure water should be used to prevent sediment formation.

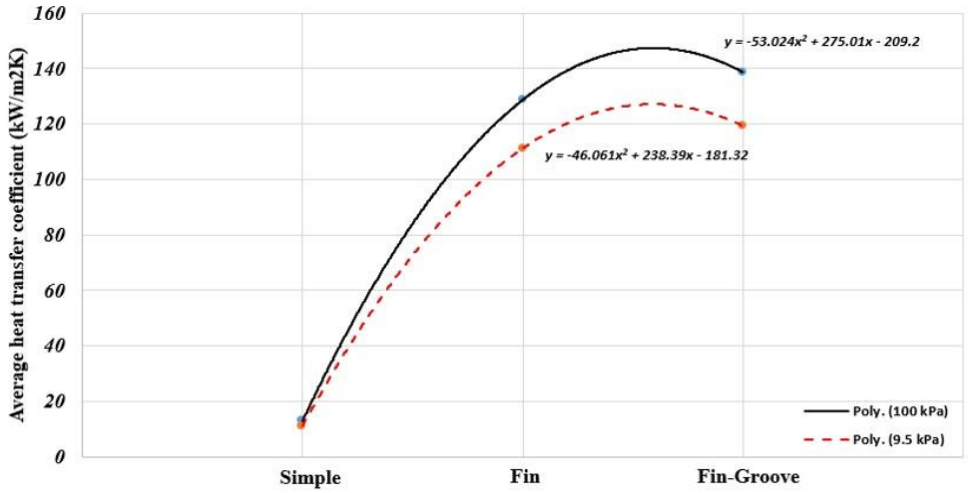

Figure 9. Average heat transfer coefficient for the three types of heat exchangers, highlighting the performance improvement due to fins and grooves.

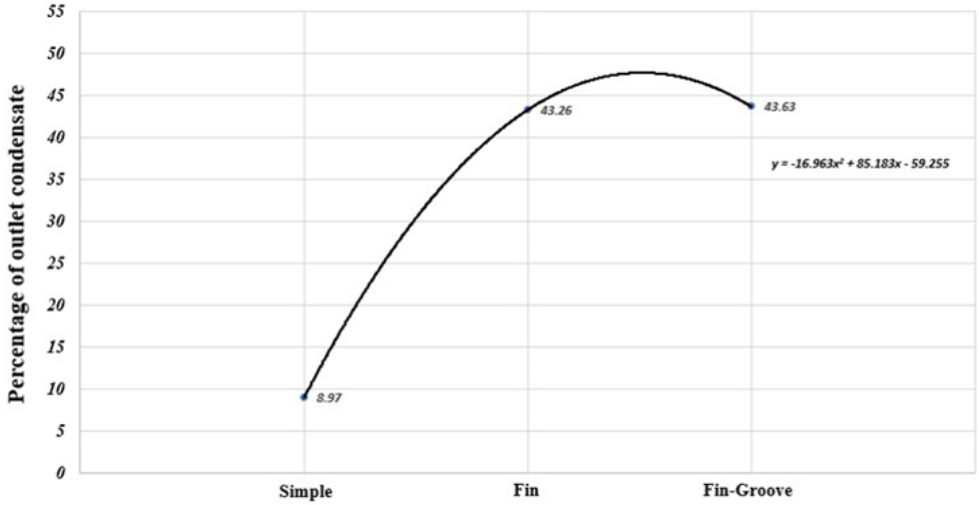

Figure 10. Percentage of outlet condensate relative to total outlet fluid for the three heat exchanger configurations

Based on achievements in this study, a comprehensive parametric optimization study, investigating the effects of varying fin and groove dimensions (e.g., height, spacing, angle) on the performance of heat exchangers were performed in another works from our team. The process of fin and groove geometry optimization involved the coupling of CFX and Design Explorer software in aforementioned study. In future studies, it is already planned to include a detailed analysis of the hydraulic performance of the heat exchangers, including pressure drop calculations and their effect on overall system efficiency. We should clarify that the reported 906% increase in heat transfer is presented with uncertainty analysis, and the physical mechanisms responsible for this enhancement are discussed in detail. Potential limitations, including increased pressure drop, fouling, and cost implications, are addressed. Future research will focus on experimental validation and parametric studies to optimize the design under realistic operational conditions. The industrial applicability of the proposed tube geometries must consider potential challenges such as increased manufacturing costs, material selection, and the impact on system design. Further analyses will be conducted to evaluate these factors in real-world applications.

In conclusion, this study compared the effect of three different types of horizontally oriented condensation systems (i.e., a simple tube, a tube with external fins, and a tube with internal grooves) on various heat transfer parameters using CFD modeling. The overall findings indicated improved performance of the heat exchangers for systems with external fins and internal grooves. These results highlight the importance of cooling tube geometry on heat exchanger performance and suggest that further studies are needed in this field. The design of fins and grooves can significantly affect the performance of heat exchangers, and determining the optimal geometry should be a focus of future investigations.

CONFLICT OF INTEREST

The authors declare that the research was conducted in the absence of any commercial or financial relationships that could be construed as a potential conflict of interest.

REFERENCES

Bonneau, C., Popov, D., Gebauer, T., Kleiner, T., Chen, J., Saleh, E. A., et al. (2019). Comprehensive review of pure vapour condensation outside of horizontal smooth tubes. Nuclear Engineering and Design, 349, 92–108. https://doi.org/10.1016/j.nucengdes.2019.04.005

Cavallini, A., Col, D., Del Col, D., Longo, G. A., & Rossetto, L. (2003). Condensation inside and outside smooth and enhanced tubes: A review of recent research. International Journal of Refrigeration, 26(4), 373–392. https://doi.org/10.1016/S0140-7007(02)00150-0

Chen, J., Sun, Z., Zhang, X., & Yan, W. (2019). Precision determination of film condensation row effect of R134a condensation on an array of horizontal plain tubes. Experimental Thermal and Fluid Science, 109, 109849. https://doi.org/10.1016/j.expthermflusci.2019.109849

Dalkilic, A. S., & Wongwises, S. (2009). Intensive literature review of condensation inside smooth and enhanced tubes. International Journal of Heat and Mass Transfer, 52(15–16), 3409–3426. https://doi.org/10.1016/j.ijheatmasstransfer.2009.01.011

Dobson, M. K., & Chato, J. C. (1998). Condensation in smooth horizontal tubes. Journal of Heat Transfer, 120(1), 193–213. https://doi.org/10.1115/1.2830043

García-Valladares, O. (2003). Review of in-tube condensation heat transfer correlations for smooth and microfin tubes. Heat Transfer Engineering, 24(4), 6–24. https://doi.org/10.1080/01457630304036

Gebauer, T., Korn, T., & Ziegler, F. (2013). Condensation heat transfer on single horizontal smooth and finned tubes and tube bundles for R134a and propane. International Journal of Heat and Mass Transfer, 56(1–2), 516–524. https://doi.org/10.1016/j.ijheatmasstransfer.2012.09.049

Ghedira, A., Saada, R., Soualmia, A., & Baccar, M. (2025). Numerical simulation of incompressible two-phase flows with phase change process in porous media. Results in Engineering, 25, 103706. https://doi.org/10.1016/j.rineng.2024.103706

Infante Ferreira, C. A., Bandarra Filho, E. P., & Pires, R. (2003). R404A condensing under forced flow conditions inside smooth, microfin and cross-hatched horizontal tubes. International Journal of Refrigeration, 26(4), 433–441. https://doi.org/10.1016/S0140-7007(02)00156-1

Kharangate, C. R., & Mudawar, I. (2017). Review of computational studies on boiling and condensation. International Journal of Heat and Mass Transfer, 108, 1164–1196. https://doi.org/10.1016/j.ijheatmasstransfer.2016.12.065

Kleiner, T., Gebauer, T., & Ziegler, F. (2019). CFD model and simulation of pure substance condensation on horizontal tubes using the volume of fluid method. International Journal of Heat and Mass Transfer, 138, 420–431. https://doi.org/10.1016/j.ijheatmasstransfer.2019.04.054

Popov, D., Kuznetsov, G., & Strizhak, P. (2019). Cryogenic heat exchangers for process cooling and renewable energy storage: A review. Applied Thermal Engineering, 153, 275–290. https://doi.org/10.1016/j.applthermaleng.2019.02.106

Rifert, V., & Sereda, V. (2015). Condensation inside smooth horizontal tubes: Part 1. Survey of the methods of heat-exchange prediction. Thermal Science, 19(5), 1769–1789. https://doi.org/10.2298/TSCI140522036R

Saleh, E. A., & Ormiston, S. J. (2016). A sharp-interface elliptic two-phase numerical model of laminar film condensation on a horizontal tube. International Journal of Heat and Mass Transfer, 102, 1169–1179. https://doi.org/10.1016/j.ijheatmasstransfer.2016.07.013

Wongwises, S., & Polsongkram, M. (2006). Condensation heat transfer and pressure drop of HFC-134a in a helically coiled concentric tube-in-tube heat exchanger. International Journal of Heat and Mass Transfer, 49(23–24), 4386–4398. https://doi.org/10.1016/j.ijheatmasstransfer.2006.05.010

Yang, L., & Shen, S. (2008). Experimental study of falling film evaporation heat transfer outside horizontal tubes. Desalination, 220(1–3), 654–660. https://doi.org/10.1016/j.desal.2007.02.046

Yang, Z., Li, D., Liang, Y., & Chen, H. (2008). Numerical and experimental investigation of two-phase flow during boiling in a coiled tube. International Journal of Heat and Mass Transfer, 51(5–6), 1003–1016. https://doi.org/10.1016/j.ijheatmasstransfer.2007.05.025

Zhang, J., Liu, Y., Wu, H., & Chen, X. (2025). Condensation heat transfer efficiency analysis of horizontal double-sided enhanced tubes. Energies, 18(9), 2390. https://doi.org/10.3390/en18092390